Molecular Therapy
Methods & Clinical Development
Original Article

C3 Transferase-Expressing scAAV2 Transduces Ocular Anterior Segment Tissues and Lowers Intraocular Pressure in Mouse and Monkey

Junkai Tan,[1,5] Xizhen Wang,[2,5] Suping Cai,[2,5] Fen He,[2] Daren Zhang,[1] Dongkan Li,[1] Xianjun Zhu,[3,4] Liang Zhou,[4] Ning Fan,[2] and Xuyang Liu[1,2]

[1]Xiamen Eye Center, Xiamen University, Xiamen, China; [2]Shenzhen Key Laboratory of Ophthalmology, Shenzhen Eye Hospital, Jinan University, Shenzhen, China; [3]Institute of Laboratory Medicine, Sichuan Academy of Medical Sciences & Provincial People's Hospital, Chengdu, Sichuan, China; [4]Institute of Laboratory Animal Sciences, Sichuan Academy of Medical Sciences & Provincial People's Hospital, Chengdu, Sichuan, China

Glaucoma is a lifelong disease with elevated intraocular pressure (IOP) as the main risk factor, and reduction of IOP remains the major treatment for this disease. However, current IOP-lowering therapies are far from being satisfactory. We have demonstrated that the lentivirus-mediated exoenzyme C3 transferase (C3) expression in rat and monkey eyes induced relatively long-term IOP reduction. We now show that intracameral injection of self-complementary AAV2 containing a C3 gene into mouse and monkey eyes resulted in morphological changes in trabecular meshwork and IOP reduction. The vector-transduced corneal endothelium and the C3 transgene expression, not vector itself, induced corneal edema as a result of actin-associated endothelial barrier disruption. There was a positive (quadratic) correlation between measured IOP and grade of corneal edema. This is the first report of using an AAV to transduce the trabecular meshwork of monkeys with a gene capable of altering cellular structure and physiology, indicating a potential gene therapy for glaucoma.

INTRODUCTION

Primary open angle glaucoma (POAG) is considered as a lifelong disease involving optic nerve deterioration with elevated intraocular pressure (IOP) as the main risk factor. Proper IOP-lowering treatments can prevent or slow down the glaucomatous retinal ganglion cell loss.[1] Even though these approaches have been successfully used for several decades, they carry a number of problems, with some potentially causing failure of the treatment. One of the most important issues is that the IOP-lowering effects of current available therapeutic strategies usually failed to last long. Although trabeculectomy and other similar surgical procedures can lower IOP by creating an additional channel to drain aqueous humor, the main complications, including scarring around the fistula, will lead to failure of the surgeries.[1,2] Therefore, alternative approaches for glaucoma treatment are in urgent need.

It is generally accepted that the actin cytoskeleton and its associated cellular interactions in the trabecular meshwork (TM) and juxtacanalicular tissue (JCT) contribute mainly to the formation of aqueous outflow resistance. Rho-GTPase (Rho)-mediated signaling pathways regulate the assembly and contractility of the actomyosin network. Rho-associated protein kinase (ROCK) is one of the major downstream effectors of Rho, and previous studies showed that the inhibition of ROCK lowers IOP in rats, rabbits, monkeys, and POAG patients.[3–7] Exoenzyme C3 transferase (C3), isolated from *Clostridium botulinum*, specifically inactivates Rho by ADP ribosylation.[8] Our previous work elucidated that adenoviral-vector-mediated C3 expression can significantly induce morphological changes in cultured human TM (HTM) cells and increase outflow facility in organ-cultured monkey anterior segments.[9] Our group also reported that C3 expressed by lentiviral vector (LV) inactivates RhoA in HTM cells by ADP ribosylation, resulting in the disruption of actin cytoskeleton and altered cell morphology, and lowered IOP in rat eyes for 40 days[10] and in monkey eyes for 112 days.[11] Interesting enough, there were no significant inflammatory reactions observed in these *in vivo* studies.[10,11]

In the present study, we investigated the possibility of developing a potential glaucoma gene therapy using self-complementary adeno-associated virus. (AAV) (scAAV) vectors. This is the first report, to the best of our knowledge, of using an AAV-based vector to transduce the TM of a live nonhuman primate with a gene capable of altering cellular structure and histology and lowering IOP. Even though the vector can efficiently transduce the corneal endothelium (CE), the vector itself did not affect the cornea. We, therefore, compared the differences of biological properties between the scAAV2 and LV used in our previous studies.

RESULTS

Effects of scAAV2-Mediated C3 Expression on HTM Cells

Recombinant scAAV2 expressing either enhanced green fluorescent protein (scAAV2-EGFP) or C3 protein (scAAV2-C3) were prepared.

Received 24 August 2019; accepted 19 November 2019;
https://doi.org/10.1016/j.omtm.2019.11.017.

[5]These authors contributed equally to this work.

Correspondence: Xuyang Liu, Xiamen Eye Center, Xiamen University, Xiamen, China.
E-mail: xliu1213@126.com

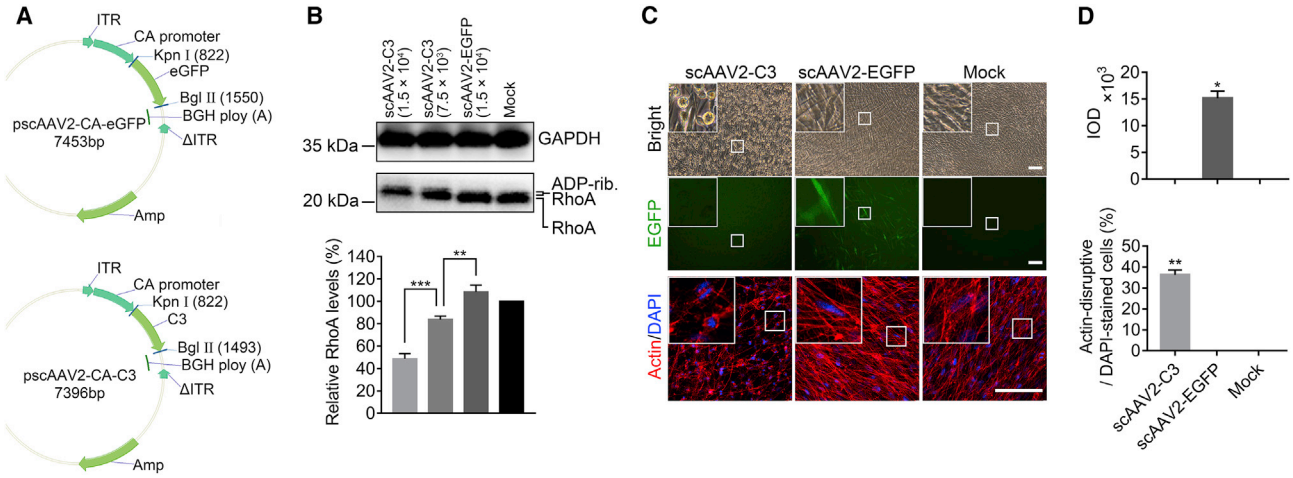

Figure 1. Effects of scAAV2-Mediated C3 Expression on HTM Cells

(A) Detailed structure of the scAAV2 vectors. ITR, inverted terminal repeat; ΔITR, truncated ITR; C3, C3 gene; EGFP, enhanced GFP gene; CA promoter, a promoter that combined the CMV enhancer with the chicken beta-actin promoter; BGH polyA, a poly(A) signal from the bovine growth hormone gene; Amp, ampicillin gene. (B) Western blot and densitometric analysis for total RhoA expression at 48 h post-vector transduction at different MOIs (1.5×10^4 and 7.5×10^3). ADP-rib. RhoA, ADP-ribosylated RhoA. Results were normalized to the reference protein GAPDH, and these values were further standardized to that value in the mock group. (C) The morphological changes, EGFP expression, and actin labeling in HTM cells at 48 h after scAAV2 vector transduction (MOI = 1.25×10^4). Scale bars, 100 μm. (D) Integrated optical density (IOD; top) and percentage of actin cytoskeleton-disruptive cells (bottom) in the three groups. The amount of cells in each field (263 μm × 263 μm) was counted in terms of DAPI-stained cells. All error bars indicate SEM, and the significance of difference was calculated using one-way analysis of variance (ANOVA). For (B), n = 3 per group; **$p < 0.01$; ***$p < 0.001$. For (D), n = 3; *$p < 0.05$ **$p < 0.01$ versus scAAV2-EGFP and mock groups.

scAAV2-EGFP-treated and medium-only-treated cells were used as viral-only and negative controls (mock), respectively. Multiplicities of infection (MOIs) were determined by simply dividing the number of viral particles (milliliters added × viral genomes [vgs] per milliliter]) by the number of cells added per well. HTM cells were cultured to an endothelial-like monolayer with extensive intercellular contacts. Compared to the controls, HTM cells transduced with scAAV2-C3 appeared to be either elongated or rounded up at 24 h, and their changes became more obvious at 48 h after exposure (Figure 1C). Correspondingly, there was a disruption of actin cytoskeleton and morphological changes in cells treated with scAAV2-C3 at a MOI of 1.25×10^4 (Figure 1C), which was not observed in controls. Quantitatively significant differences in actin cytoskeleton disruption were detected among these three groups (Figure 1D, bottom; n = 3; $p < 0.01$). The bright EGFP expression was found in the scAAV2-EGFP-treated cells but was not detected in the scAAV2-C3-treated cells or the mock cells (Figures 1C, middle, and 1D, top).

As C3 modifies and inhibits Rho, RhoA expression in HTM cells was examined by western blot following C3 expressing vector delivery. The results (Figure 1B) showed an increase in the molecular weight of RhoA, which was presumably due to the ADP ribosylation of the protein and a significant decrease in RhoA level in the scAAV2-C3 group, consistent with previous studies, including ours.[11,12] These changes were in a dose-dependent manner, with maximum changes observed with a MOI of 1.5×10^4 of scAAV2-C3, showing a band with a slightly increased molecular weight and the RhoA level reduced by 51% (Figure 1B; n = 3, $p < 0.001$; versus scAAV2-EGFP, $p < 0.001$ versus mock). There was no difference observed between scAAV2-EGFP-treated and mock cells ($p > 0.05$).

EGFP Expression in Anterior Segments Following Vector Delivery

C57BL/6 mice were injected in one eye with 5×10^8 vgs of either scAAV2-C3 or scAAV2-EGFP, and the fellow eye served as the normal control (un-injected). For each *Macaca mulatta* rhesus monkey, a single dose of 3×10^{10} vgs of scAAV2-C3 was injected intracamerally into one eye, and the same dose of scAAV2-EGFP was injected into the contralateral eye.

Mice injected intracamerally with scAAV2-EGFP showed positive fluorescence mainly in the anterior chamber angle and the CE at day 14 after injection (Figure 2A). In monkey eyes, because the nasal anterior chamber angle was covered by epicanthus, the temporal quadrant was used as the main region for fluorescence detection. Monkey eyes receiving scAAV2-EGFP demonstrated detectable EGFP expression in the tissues of the anterior chamber angle as early as 3 days post-injection (Figure 2C). The dust-like fluorescence was distributed in the anterior chamber and was more obviously visible at 14, 35, 70, and 77 days when the examination under anesthesia was performed. A starry fluorescence was found over all the quadrants of the CE (Figures 2C and 2D). All scAAV2-C3-injected eyes demonstrated no EGFP expression at each time point.

To investigate whether the EGFP expression *in vivo* was on the CE of mouse, the corneal flat mounts were used to detect the fluorescence

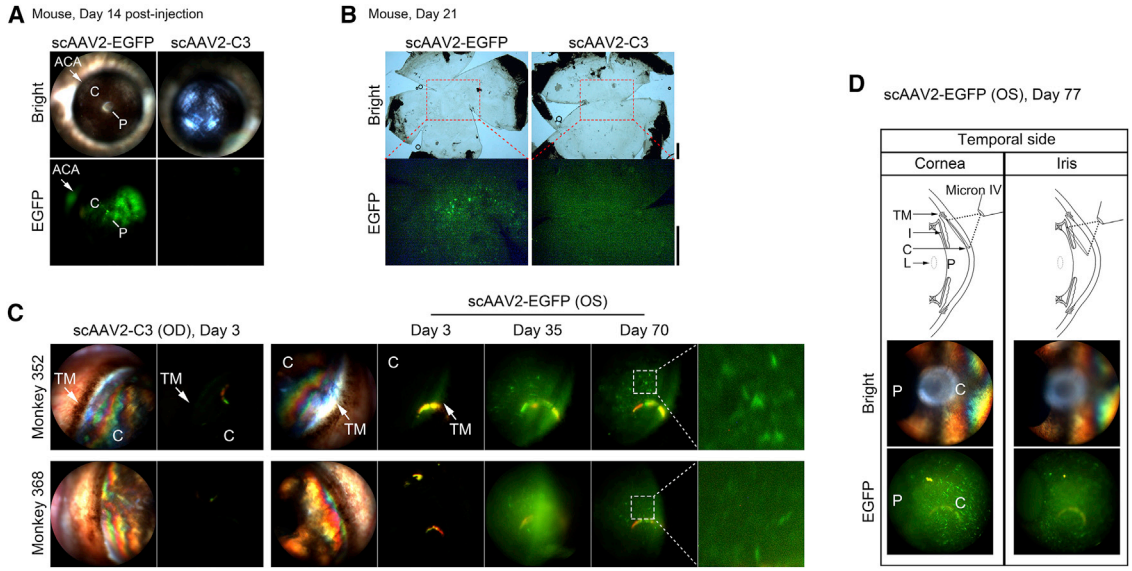

Figure 2. EGFP Expression in the Anterior Segment of Animals

(A, C, and D) *In vivo* light and fluorescence images were captured by Micron IV. (A) EGFP expression of whole anterior segment at 14 days after scAAV2 vector injection. Arrows indicate fluorescence in the anterior chamber angle (ACA). (B) Fluorescence images of postmortem mouse flat-mount cornea obtained at 21 days after scAAV2 vector transduction (taken with an Olympus CKX53 microscope). Scale bar, 500 μm. (C) EGFP expression in temporal quadrant of monkeys 352 and 368 at 3, 35, and 70 days after injection with scAAV2 vectors. Arrows indicate fluorescence in the region of the trabecular meshwork (TM). (D) Top: schematic diagram showing the way to distinguish whether the fluorescence was located in the corneal endothelium or on the anterior surface of the iris. Middle and bottom: EGFP expression of these areas in the temporal quadrant at 77 days after injection with scAAV2-EGFP. OS, left eye; OD, right eye; C, cornea; P, pupil; L, lens.

postmortem. As observed in the living mice at 14 days, the CE appeared highly fluorescently labeled 21 days after transduction (Figure 2B).

To identify whether scAAV2 transduction was located on the CE of monkey, the clarity of the fluorescence image of this region was evaluated when the Micron IV focused on the cornea. As shown in Figure 2D, there were clearly sporadic signals in the CE when the Micron IV focused on the cornea, whereas the fluorescence image of the CE was blurry when the Micron IV focused on the iris, strongly indicating that the scAAV2 transduction was located on the CE instead of the anterior face of the iris, consistent with a previous report.[13]

Monitoring Inflammatory Reactions in the Anterior Segments

The corneal edema is graded as previously described: grade 0 is defined as no edema; grade 1, as slight edema with clear view of iris details; grade 2, as edema with clear view of pupil details; grade 3, as edema with obscuring view of pupil details; and grade 4, as dense edema with epithelial microcystic edema and obscuring pupil detail.[11]

Mouse eyes injected with scAAV2-EGFP showed neither opacity nor signs of inflammation during the experiment, but those injected with scAAV2-C3 exhibited corneal edema of grade 2 at day 7 post-injections (Figure 3A).

Table 1 summarizes the clinical observations in monkey eyes. Monkeys intracamerally injected with scAAV2-EGFP showed neither signs of inflammation nor opacity in the anterior segment of the eyes (Figures 3B and 3C; Table 1). The scAAV2-C3-transduced eyes were clear until 7 days post-transduction and then developed a corneal edema at different grades. Two monkeys presented with a corneal edema of grade 1 (monkeys 309 and 285), and another two presented with a corneal edema of grade 2 (monkeys 346 and 352). After that, the corneal edema in those four monkeys were more obvious until 63 days (Figure 3D; Table 1), when the corneal edema of grade 4 was found in monkey 352, that of grade 3 was found in monkey 346, and that of grade 2 was found in monkeys 285 and 309. Monkey 368 showed a mild cornea edema (less than grade 1) on day 14, and no significant changes observed thereafter. Other than corneal edema, no other signs or abnormalities were observed in these scAAV2-C3-transduced eyes.

IOP Changes in Animals Transduced with scAAV2 Vectors

In mice, the pretreatment IOP (baseline) was 12.67 ± 0.24 mmHg and 13.08 ± 0.42 mmHg in eyes to be injected with scAAV2-C3 and scAAV2-EGFP, respectively (n = 4 for each group), and there was no significant difference in baseline between the two groups ($p > 0.05$). The IOP in the scAAV2-EGFP-treated eyes did not showed significant change at day 7 post-injection, when compared to the baseline (Figure 4A; $p > 0.05$), with a mean percent IOP reduction of 2.3% ± 3.1% corresponding to a mean IOP difference of 0.33 ± 0.41 mmHg. However, scAAV2-C3 significantly lowered IOP in mice at day 7 after injection, when compared to the baseline (Figure 4A; $p < 0.01$), with a mean percent IOP reduction of

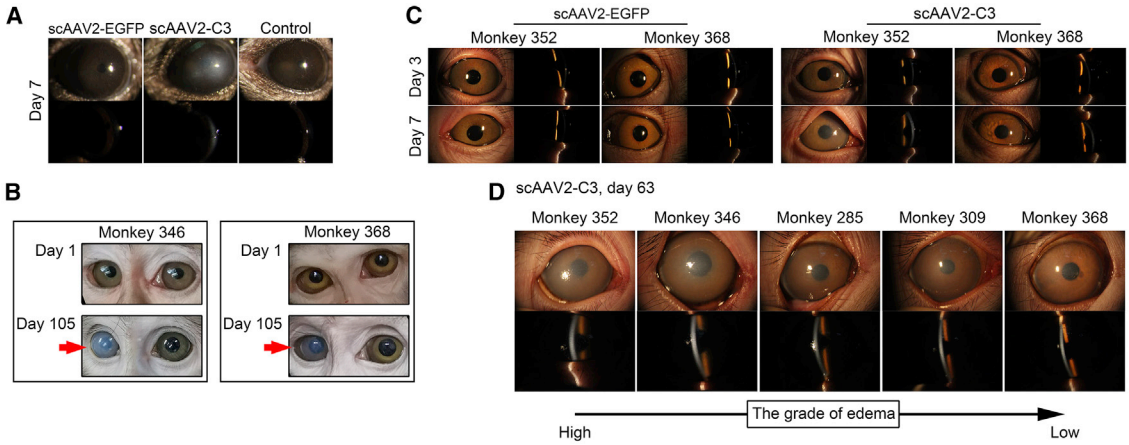

Figure 3. Slit-Lamp Examination

(A) Representative images of anterior segments of mouse eyes at day 7. (B–D) Representative images of anterior segments of monkey eyes at different time points, including the general status at days 1 and 105 (B), and the slit-lamp examination at days 3 and 7 (C) and day 63 (D). Red arrows indicate corneal opacity presented in scAAV2-C3-injected monkey eyes (right eye). (D) The images of anterior segment are presented in descending order by severity of corneal edema at day 63 post-scAAV2-C3 injection (from left to right).

18.4% ± 1.6% corresponding to mean IOP difference of 2.33 ± 0.24 mmHg. There was a significant difference at day 7 in the mean percent IOP reduction between the scAAV2-C3-treated and scAAV2-EGFP-treated eyes (Figure 4A; $p < 0.01$).

Effects of the intracameral injection of scAAV2-C3 or scAAV2-EGFP on IOP of monkeys are shown in Figures 4B and 4C. The pretreatment IOP was 14.13 ± 0.42 mmHg and 14.00 ± 0.38 mmHg in eyes to be injected with scAAV2-C3 and scAAV2-EGFP, respectively ($n = 5$). There was no statistical difference in the baseline values of IOP between the two groups ($p > 0.05$). The IOP in the scAAV2-EGFP-treated eyes did not show significant changes post-treatment when compared to baseline (Figure 4B; $p > 0.05$). scAAV2-C3 significantly lowered IOP in monkey eyes at days 3, 7, 14, and 21 after injection, when compared to the baseline (Figure 4B; $p < 0.05$). As an example, there was a mean percent IOP reduction of 35.1% ± 6.3% corresponding to a mean IOP difference of 4.93 ± 0.85 mmHg at day 7. At days 3, 7, and 14, there were significant differences of mean percent IOP reduction between the scAAV2-C3 and scAAV2-EGFP groups (Figure 4B; $p < 0.05$).

To delineate the difference of IOP response in each monkey, the post-treatment IOPs were corrected for baseline IOP (IOP ratio) and charted as shown in Figure 4C. All IOP ratios in the scAAV2-EGFP group (IOP ratios-EGFP) showed a slight fluctuation around the baseline (IOP ratio = 1), while IOP ratios in the scAAV2-C3 group (IOP ratio-C3) exhibited a gradient difference among monkeys. After 28 days, the IOP ratio-C3 persisted below or above 1 in monkey 368 and monkey 352, respectively. Except for a few time points, the IOP ratio-C3 in monkeys 309 and 346 mainly stayed below or above 1, respectively. The changes in the IOP ratio-C3 in monkey 285 were between those of other monkeys and fluctuated around 1 until euthanasia. Furthermore, the status of the IOP ratio-C3 below 1 was kept until day 301 in monkeys 368 and 309.

Ultrasound Biomicroscopy (UBM) Examination and Corresponding Quantification of Central Corneal Thickness (CCT)

UBM allows the assessment *in vivo* of the anterior segment morphology and the CCT measurement in monkey eyes (Figure 4D). Compared to the scAAV2-EGFP group (490.5 ± 4.2 μm), the CCT significantly thickened in the scAAV2-C3 group (1,136.0 ± 89.6 μm) at day 175 post-injection ($n = 4$; $p < 0.01$). The CCT of the scAAV2-C3-transduced eye was corrected by contralateral CCT and presented as the CCT ratio-C3/EGFP. The CCT ratios-C3/EGFP were significantly different among monkeys at the same dose of C3 transduction ($p < 0.001$) and presented in the following order: monkey 352 (2.84 ± 0.04) > monkey 346 (2.38 ± 0.03) > monkey 309 (2.16 ± 0.03) > monkey 368 (1.91 ± 0.04).

The Impact of Corneal Edema on IOP Measurements

Analysis of the results of IOP measurements and slit-lamp examinations performed at 15 time points from day 0 to day 126 showed that there was a potential relationship between IOP ratio and grade of corneal edema in the monkey eyes. A quadratic relationship was found between IOP ratio and the grade of corneal edema (Figure 4E; $r^2 = 0.50$, $p < 0.001$). When the grade was over 1, the level of corneal edema showed a positive correlation with the IOP measurements.

Since there was no significant difference of CCT between the right and left eyes in either adult or infant monkeys as previously described,[14] it is therefore assumed that, for each monkey, the CCTs of both the eyes to be injected with scAAV2-EGFP (right eye) and the scAAV2-C3-injected eye (left eye), respectively, were not different on day 0. The scAAV2-EGFP-injected eyes demonstrated normal signs at each time point; thus, the CCTs of those

Table 1. Summary of Clinical Observation Assessed in Anterior Segments

Monkey and scAAV2-Mediated Expression	Eye	Grade of Corneal Edema		
		Day 3	Day 7	Day 63
352				
EGFP	OS	0	0	0
C3	OD	0	2	4
346				
EGFP	OS	0	0	0
C3	OD	0	2	3
285				
EGFP	OS	0	0	0
C3	OD	0	1	2
309				
EGFP	OS	0	0	0
C3	OD	0	1	2
368				
EGFP	OS	0	0	0
C3	OD	0	0	1

Monkeys were administered a dose of 3×10^{10} vgs. There were no other signs, including hyperemia, conjunctivitis, and flare. OS, left eye; OD, right eye.

eyes at day 175 were equal to the CCTs of ipsilateral eyes at day 0. That is, the CCT ratio of before and after scAAV2-EGFP transduction (CCT ratio-EGFP) was 1, and the CCT ratio of scAAV2-C3-injected and scAAV2-EGFP-injected eye (CCT ratio-C3/EGFP) was equal to the CCT ratio of before and after C3 transduction (CCT ratio-C3). When the results of IOP response and CCT measurement were analyzed at 2 time points (day 0 and day 175), there was a quadratic relationship between IOP ratio and CCT ratio ($r^2 = 0.78$, $p < 0.001$). The CCT was positively correlated with measured IOP when the CCT ratio was over 1.6 (Figure 4F).

Hematoxylin and Eosin (H&E) Staining and Actin Labeling in the Anterior Segment of Animals

In H&E-stained paraffin sections, the histology of the anterior segment was analyzed in mouse and monkey eyes (Figures 5A–5E). Mouse eyes transduced with scAAV2-C3 exhibited a significant corneal thickening (155.3 ± 5.9 μm) at day 21, when compared to the scAAV2-EGFP-transduced eyes (Figure 5A, top; 97.0 ± 1.8 μm; $n = 3$; $p < 0.001$). Vacuoles were found on the posterior face of the iris in the scAAV2-C3-transduced mouse eyes, but not in the scAAV2-EGFP-transduced mouse eyes (Figure 5A, middle). The scAAV2-C3-treated mouse eyes showed greater intertrabecular space in the TM than scAAV2-EGFP-treated eyes (Figure 5A, bottom). In monkey 285, the scAAV2-C3-transduced eye showed an edematous corneal stroma with blurring borders of collagen fiber in the posterior layer (Figure 5B), and the contracted endothelium was detached from Descemet's membrane (Figure 5C). There were vacuoles observed on the posterior face of the iris of C3-transduced monkey eye (Figure 5D). All tissues of anterior segment showed no abnormalities in the scAAV2-EGFP-transduced monkey eye. In the TM (Figure 5E), the scAAV2-EGFP-transduced eye exhibited the regular organization of the beams and compact JCT, while the scAAV2-C3-transduced eye exhibited disorganized beams, loose stroma, and widened spaces within the JCT and TM. No inflammatory cell infiltration or proliferation was found in both scAAV2-EGFP-transduced and scAAV2-C3-transduced eyes.

Changes in the TM of monkey eye were also evaluated by phalloidin labeling of actin (Figure 5G). Compared to the scAAV2-EGFP group, there were contracted cells, discontinuity of intercellular junctions, and widening of intertrabecular spaces and the empty areas within the JCT and TM in scAAV2-C3-injected eye. In the CE of mouse flat-mount cornea (Figure 5F), the distribution of phalloidin labeling actin was concentrated in the circumferential cytoplasm. The mouse CE transduced with scAAV2-EGFP showed confluent hexagonal endothelial cells, an oval nucleus, and intact intercellular junctions, while scAAV2-C3-transduced CE demonstrated cavities scattered over the whole layer, contracted nucleus, and disorganized cell morphologies.

The Changes in Ultrastructure of CE in Monkey 285

Transmission electron microscopy (TEM) (Figure 5H) showed that the monolayer of endothelium was arranged tightly on Descemet's membrane in the scAAV2-EGFP-injected monkey eye. The endothelial cells with an oval nucleus were tightly attached to each other, and the intercellular borders did not appear to be distinct. In the scAAV2-C3-transduced CE, the cells lose their intercellular and cell-basement junctions. The contracted endothelial cells were detached from Descemet's membrane and exhibited the distinct cell borders. The intact cell nuclei were found in either the scAAV2-EGFP-transduced or the scAAV2-C3-transduced CE.

DISCUSSION

The modulation of IOP is crucial for the eye, and its elevation remains the major risk factor for the pathogenesis of glaucoma. Increased IOP is mainly due to the abnormally increased resistance to aqueous humor in the regions of the TM and JCT, as observed in some glaucoma patients.[15–17] It is known that the actin cytoskeleton and its associated cellular interactions regulated by the Rho/ROCK pathway play a crucial role in the formation of resistance to outflow and IOP modulation of the eye. A number of studies, including ours, have demonstrated that ROCK inhibitors, such as Y-27632, H-1152, and ripasudil (K-115), increased outflow facility and reduced IOP in rats, rabbits, monkeys, and human patients.[3–7] Therefore, the inhibition of the Rho/ROCK pathway is able to change the resistance of the TM and JCT to the outflow and, as a result, lower the IOP. Previous studies showed that the downregulation of 14-3-3 zeta resulted in the inhibition of transforming-growth-factor-β1 (TGF-β1)-induced contraction by decreasing the RhoA expression in HTM cells.[18] RhoA-induced ocular hypertension in a rodent model was associated with increased fiborgenic activity,[19] and the small interfering RNA against RhoA suppressed the TGF-β-induced early IOP elevations in rats.[20] Furthermore, a dominant-negative mutant RhoA delivered

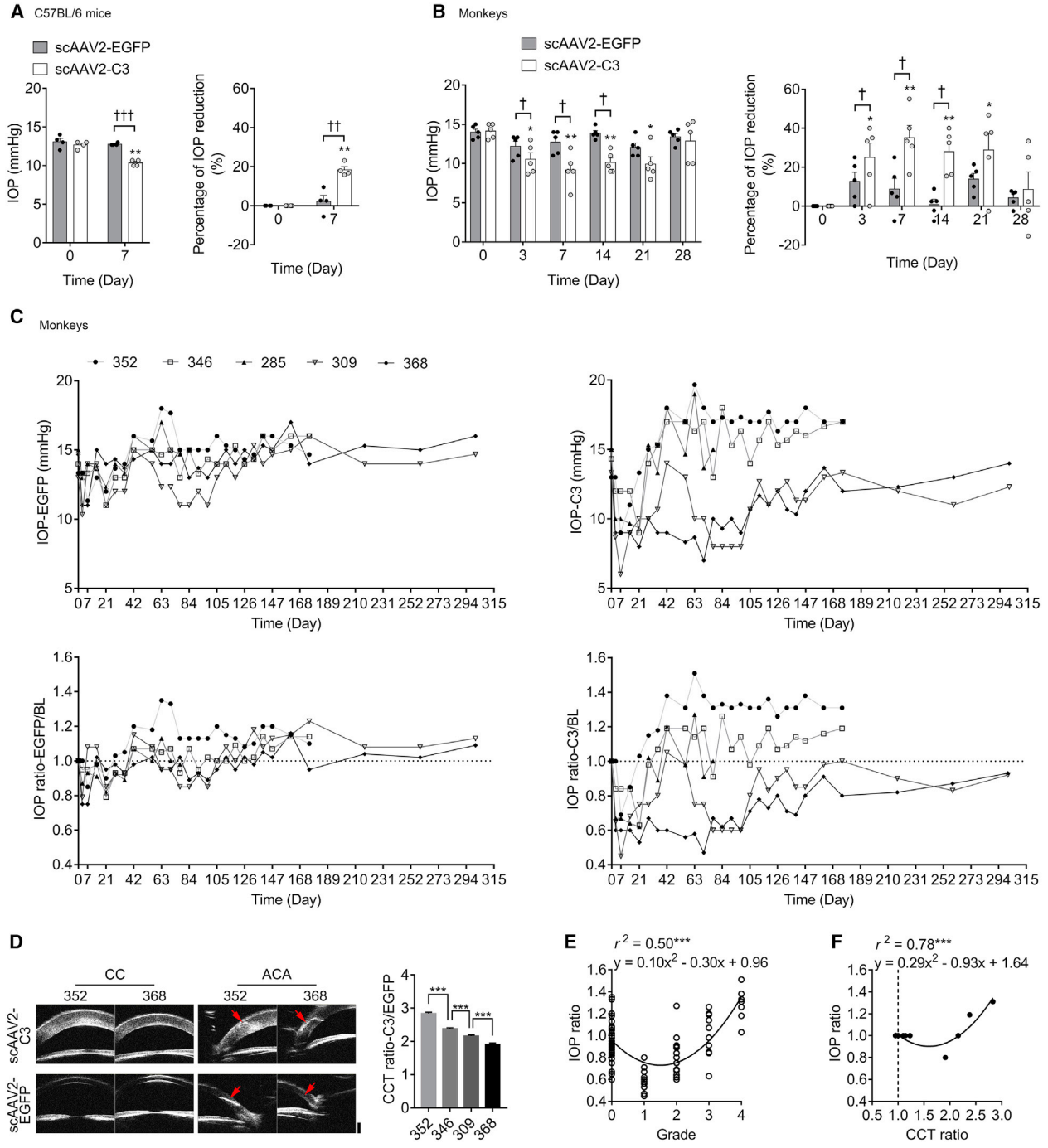

Figure 4. The IOP Changes from Baseline after Vector Delivery and the Correlation of IOP Ratio and Grade of Corneal Edema or CCT Ratio

(A) Mean IOP percent changes in mouse eyes before (day 0) and after (day 7) vector transduction (n = 4). (B) Mean IOP percent changes in monkey eyes before (day 0) and after (days 3, 7, 14, 21, and 28) vector transduction (n = 5). Error bars represent SEM, and the statistical significance in mean IOP percent changes was calculated using the two-tailed paired t test. *$p < 0.05$ and **$p < 0.01$ versus baseline; $^{\dagger}p < 0.05$, $^{\dagger\dagger}p < 0.01$, and $^{\dagger\dagger\dagger}p < 0.001$. (C) Time course of IOP changes in each monkey after scAAV2-EGFP or scAAV2-C3 injection. The horizontal dashed line indicates no difference in IOP before and after scAAV2 vector injection (baseline; IOP ratio = 1.0). n = 5 from day 0 to day 77. n = 4 from day 77 to now. (D) Representative UBM images and corresponding CCT analysis at day 175 post-injection. The red arrows represent the site of anterior chamber paracentesis in the temporal side of cornea for vector delivery. CC, central cornea; ACA, anterior chamber angle. Scale bar, 1,000 μm. Error bars represent SEM (n = 5), and the significance of difference among the four monkeys was calculated using one-way ANOVA. (E and F) Regression analysis between the IOP ratio and the grade of corneal edema (E) and between the IOP ratio and CCT ratio (F). ***$p < 0.001$.

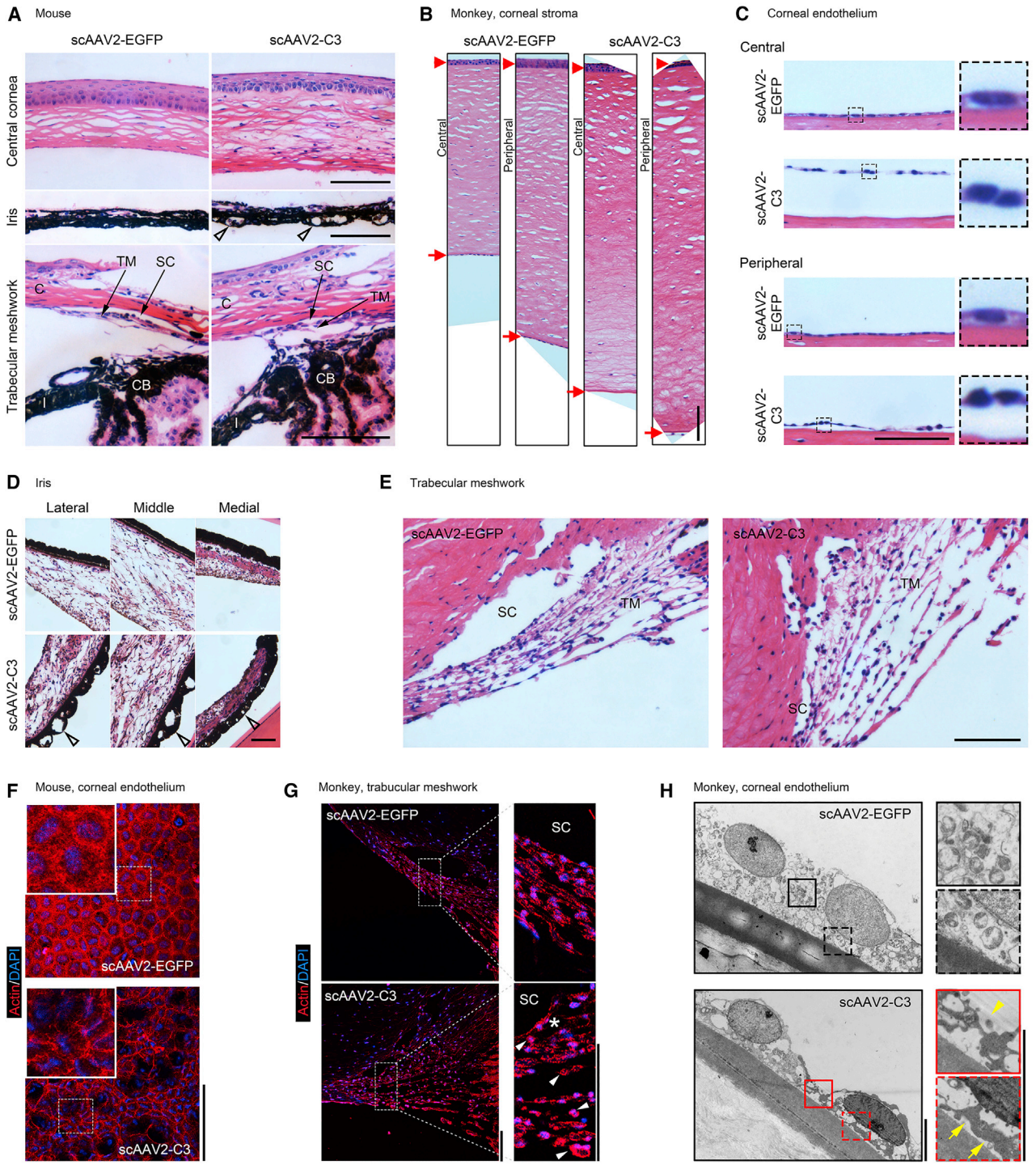

Figure 5. Histological Analysis of Anterior Segment Tissues in Mice and Monkey 285, and TEM Examination of Corneal Endothelium in Monkey 285, following Vector Treatment

(A–E) H&E staining of sections at the anterior segment from mice and monkey 285. (A) Representative images of anterior segment in mice at 21 days. C, cornea; SC, Schlemm's canal; TM, trabecular meshwork; CB, ciliary body; I, iris. (B–E) Morphological changes of anterior segment tissues, including whole cornea (B), corneal endothelium (C), iris (D), and TM (E), in monkey 285 at 77 days. Open arrowheads indicate the vacuolation on the posterior face of iris. Red arrowheads and arrows indicate the

(legend continued on next page)

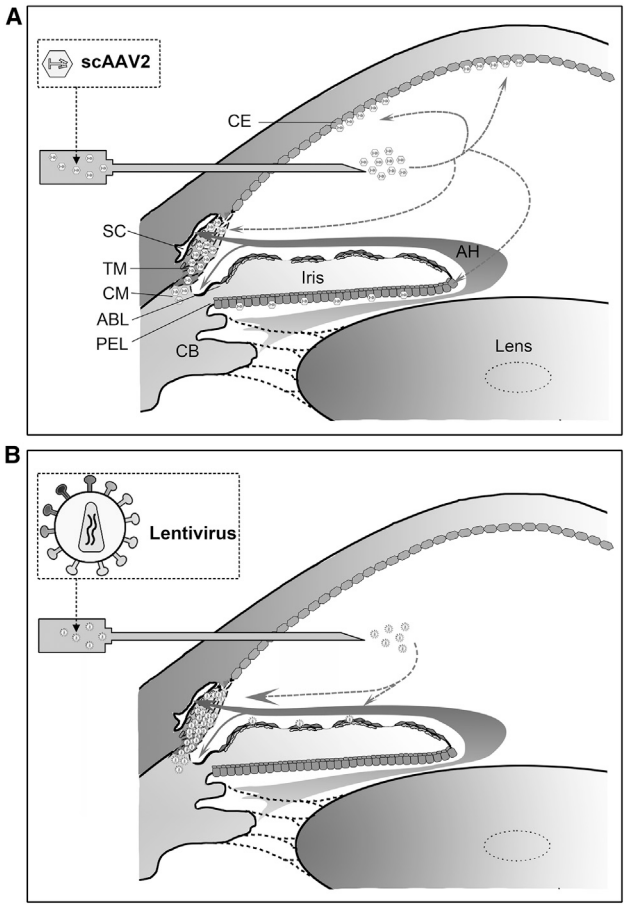

Figure 6. Schematic Diagram Showing the Capability of Two Vectors to Transduce Different Cells in the Monkey Anterior Segment after Intracameral Injection

(A and B) scAAV2 vectors (A) had a high tropism for the cells of the TM, corneal endothelium (CE), posterior epithelial layer (PEL), and ciliary muscle (CM),[13] while LVs (B) had a high tropism almost exclusively on the TM.[11,25] SC, Schlemm's canal; ABL, anterior border layer; CB, ciliary body; AH, aqueous humor.

by an adenoviral vector increased outflow facility in a human anterior segment perfusion model.[21] A scAAV2 vector expressing the mutant RhoA cDNA prevented elevation of nocturnal IOP in rats for at least 4 weeks.[22] However, the inhibition of RhoA was accompanied by a massively increased RhoB expression, which partially compensated for the cellular functions of RhoA.[23] C3, a 24-kDa single-chain protein from *Clostridium botulinum*,[8] avoids this compensation by inhibiting all Rho isomers, including RhoA, RhoB, and RhoC. We have demonstrated that an adenoviral vector was used to deliver C3 into the anterior chamber of organ-cultured monkey anterior segments and significantly increased outflow facility.[9] Furthermore, LV-mediated C3 expression induced changes in the morphology and actin cytoskeleton of cultured HTM cells, and intracameral delivery of LV-C3-GFP lowered IOP in rats[10] and monkeys[11] for at least 40 days and 112 days, respectively.[9–11] In the present study, we investigated the effects of a C3-expressing scAAV2 vector on HTM cells and on IOP in mice and monkeys and discussed the tissue tropism of this vector after delivery to the anterior chamber of monkey eyes.

Efficient reporter gene delivery to the TM of living monkey eyes[10,13,24–27] and perfused human anterior segments[28–33] was achieved by vectors derived from adenovirus,[24,28,31,32] herpes simplex virus,[27] LV[10,25,26,29,30] and scAAVs.[13,33] The schematic in Figure 6 summarizes our results and those from literature regarding the transduction ability of LV- and scAAV-based vectors in different cells and tissues of the monkey anterior segment after intracameral injection. In our previous studies,[10,11] a bright fluorescent ring was visualized in the TM following LV-mediated GFP gene transfer, and its intensity of fluorescence was much stronger than that of other tissues in anterior chamber, such as iris. Similar results were reported in cultured human donor eyes[29,30] and monkey eyes[25,26] after LV-mediated report gene transduction. The single-stranded AAVs (ssAAVs) have been used in therapy for inherited retinal and optic nerve diseases.[34,35] However, the transduction efficiency of conventional AAVs in the TM seems very low, because it is hard for AAVs to form double-stranded DNA by themselves.[33] scAAV2 is modified to bypass the required second-strand DNA synthesis. The vector shows lower immunogenicity and efficient transduction in the TM of monkeys[13] and cultured human anterior segments.[33]

Similar to our results, intracameral delivery of the scAAV2 vectors (containing cytomegalovirus [CMV] promoter in most of these studies) transduced not only the TM but also the CE and iris in live animals, including mice,[36] rats,[13,22,36,37] sheep,[38] and monkeys,[13] without inducing an inflammatory response and other abnormalities. Gruenert et al.[39] reported that the scAAV2 (CMV promoter)-transduced human corneal endothelial cells in culture maintained cellular viability and showed regular morphology. Buie et al.[13] found that one of three monkeys developed an obvious anterior chamber inflammation at 48 days after injection of the scAAV2 containing a CMV-driven GFP at a dose of 3×10^{10} vgs, suggesting that the disappearance of the GFP expression (at 70 days) was probably due to the immunogenicity of GFP but not scAAV2 itself. We injected the same dose (3×10^{10} vgs) of scAAV2 containing a CMV-driven EGFP into the monkey eyes and found a clear anterior chamber and no signs of inflammation at any time point. Although the mechanism about clinical sign differences were not clear, our findings indicated that at least the scAAV2 vector itself used in this study and the expressed EGFP are relatively safe.

corneal epithelium and endothelium, respectively. (F and G) Actin labeling on the corneal endothelium of mice (F) and the TM of monkey 285 (G). Asterisk denotes the widened spaces within juxtacanalicular tissues. White arrowheads indicate the representatively contracted cells. (H) Ultrastructural changes of the corneal endothelium on monkey 285. The C3-transduced corneal endothelium shows the loosening or separation of the cell-cell (yellow arrowheads) and cell-basement (yellow arrows) junctions. Scale bars: 100 μm in (A)–(G) and 5 μm in (H).

Even if GFP is probably immunogenic in viral-transduced monkeys as mentioned earlier, we did not notice the C3 (or EGFP-)-induced toxicity after intracameral[9–11] or intravitreal[40] injection at certain dosages or transduction units, based on our previous studies, this study, and ongoing studies (data not shown). Similar to its effects on actin cytoskeleton and cellular adhesions of the TM, the transgene expression of C3 induced the same changes in these tissues. For the iris, C3 caused vacuolation of the posterior face but failed to cause further obvious side effects, at least in the period of the experiment. For the CE, however, C3 induced contraction of endothelial cells and detachment of the cells from the basement, which, in turn, caused dysfunction of the cells and edematous cornea. In studies with a CNS injury model, C3 inactivates RhoA and, thus, promotes axon regeneration of crushed optic nerve[41–45] or traumatic spinal cord[46] without noticed inflammation or toxicity. On the contrary, other studies suggested that the Rho/ROCK signaling pathway plays a critical role in lipopolysaccharide-induced inflammation[47–49] or trauma-induced innate immune response,[50] and C3 did prevent these effects by inhibiting the release of inflammatory factors or chemotactic recruitment of monocytes. Our study also showed that the anterior chamber tissues did not exhibit inflammatory cell infiltration or proliferation after scAAV2-C3 injection. Furthermore, TEM showed an intact nucleus in the contracted endothelial cells, suggesting that C3 did not induce cell apoptosis or death.

As noted earlier, the scAAV2 vectors containing the transgene driven by a CMV promoter did not induce inflammation or toxicity in anterior chamber tissues of living animals after intracameral injection. Xiong et al.,[51] however, demonstrated that ocular toxicity after subretinal injection of ssAAVs is associated with certain *cis*-regulatory sequences, and retinal damage occurs due to the activating of glial cells and upregulation of inflammatory factors. Interestingly, this study also claimed that the toxicity had almost nothing to do with transgene expression. Therefore, it should be noted that AAV may cause toxicity. As a vector used for gene therapy purpose, no doubt, more attention should be paid not only to its properties, such as serotypes, but also to its process of preparation and purification, dose usage, and delivery procedures.

In addition, IOP-lowering effects were still present in three of these monkeys with remarkable edematous corneas after quadratic correlation between measured IOP and grade of corneal edema or CCT. The other two monkeys exhibited comparatively mild corneal edema, and the IOP-lowering effects lasted for more than 10 months. These results demonstrated the efficacy of scAAV2-mediated C3 gene therapy for IOP-lowering purposes; clearly, further studies are needed to modify the vector and avoid its tropism to unwanted ocular tissues. For monkey eyes, when compared to the LVs used in our previous studies, the latter almost significantly transduced the TM only and reduced IOP for 112 days,[11] whereas the IOP-lowering effect of the scAAV vector lasted obviously much longer.

The fluorescence was distributed as a starry sky or cluster over all quadrants of the CE in scAAV2-EGFP-injected eyes. Accordingly, corneal edema and thickening were observed in the scAAV2-C3-injected eyes after 7 days, and a quadratic relationship was found between the results of measured IOP and the grade of edema or CCT. The TonoVet tonometer uses rebound tonometry to measure IOP,[52] and there was a significant influence of corneal thickness on this type of tonometer.[53,54] Our results agree with these findings and showed a significantly positive association found between the CCT and measured IOP when the CCT ratio exceeds a value of 1.6 (Figure 4F). In addition, the severity of corneal edema seems to be of importance for its effect on tonometry using TonoVet,[55] and that relationship in our result showed an insignificant change of IOP ratio in slightly swollen corneas (grade 1 and a value of 1.6). Neuburger et al.[56] reported that the rebound tonometer yielded the accurate IOP values in human donor eye with mild edema, which may be due to their relatively small contact area with the corneal surface. Therefore, the measured IOP reduction during the mild corneal edema, such as the significant IOP reduction at days 3, 7, 14, and 21, and the long-term IOP-lowering effect in two monkeys (monkeys 309 and 368) could be close to the "true" IOP changes. A change in corneal rigidity associated with the variation in corneal water content is the likely cause of the IOP measurement inaccuracy.[57] In the monkeys 352 and 346, their measured IOPs were persistently higher than baseline (Figure 4C; the IOP ratio persistently above a value of 1), and the clinical examination showed a more obvious corneal edema compared to other monkeys. These suggest that the IOP-lowering effect of those monkeys was truly present, but the corneal edema masked this effect and caused the overestimation of TonoVet tonometer measurement.

Quick onset of the IOP-lowering effect was observed at day 3 post-injection, both in scAAV2-C3-injected and LV-C3-injected[11] monkey eyes. However, the scAAV2-C3-treated HTM cells in culture exhibited morphologic changes at 24 h, while the LV-C3-treated cells showed changes as early as 3 h. Since we cannot ensure how the IOP changes in the monkey eyes on the first and second days, these *in vitro* results indicated that the LV-based vectors result in earlier onset of C3 transgene expression than scAAV2-based vectors as evidenced by the morphological changes in cultured HTM cells. Buie et al.[13] reported that scAAV2-GFP transduced the TM very efficiently and that the reporter transgene expression lasted for at least 2.35 years in monkey. In the present study, we showed that the scAAV2-C3-induced IOP reduction occurred quickly, with durations of up to 10 months. LV transduced the TM of living monkeys, and the period of report gene expression lasted for at least 1.25 years.[25] Unexpectedly, a study using feline immunodeficiency virus (FIV)-mediated prostaglandin F synthase expression in ciliary muscle achieved 2 mmHg of IOP reduction, but the effect lasted for only 5 months in monkey eyes.[26] Similarly, the LV-C3-transduced monkey eyes demonstrated a significant IOP-lowering effect for about 4 months, as we previously reported.[11] These results indicated that the duration transgene expression of scAAV2 vector was much longer than that of LV. Therefore, scAAV2 appeared to be more promising in the use for IOP-lowering gene therapy, but again, its tropisms to the CE should be eliminated.

In summary, this finding is consistent with those of our previous studies,[9–11] showing that viral-vector-mediated C3 expression induces ADP ribosylation of RhoA, disrupts the actin cytoskeleton in HTM cells, and decreases IOP in animals. Although the TonoVet-measured lowering effect of IOP was masked by corneal edema, the measured IOP reduction was significant at days 3, 7, 14, and 21 in all monkeys, and this effect lasted for 10 months in monkeys 368 and 309 with mild cornea edema. However, scAAV2 vector shows a strong tropism in other tissue or cells (mainly in the CE) in the anterior segment of the eye; therefore, the C3 expression induced additional results, including corneal edema and iris vacuolation. Even though the scAAV2 itself did not exhibit toxic or side effects on cornea, as a vector to be used for gene therapy for lowering IOP, the vector still needs to be modified to remove its tropism to ocular tissues other than those in outflow pathways. The most commonly used primate model with elevated IOP or glaucoma can be made by application of an argon laser to part of the TM.[58] Further studies are needed to test the effect of viral vector-mediated C3 expression in ocular hypertensive primate models. The more significant IOP-lowering effects may be achieved with such models, since the reduction of IOP via trabecular meshwork pathway is pressure dependent.[59] These studies will pave the way for clinical application of glaucoma gene therapy in the future.

MATERIALS AND METHODS

Animals

All animals were maintained and handled in accordance with the Association for Research in Vision and Ophthalmology (ARVO) Statement for the Use of Animals in Ophthalmic and Vision Research. Study protocol was approved by the Institutional Animal Care and Use Committee of the Institute of Laboratory Animal Sciences, Sichuan Academy of Medical Sciences & Sichuan Provincial People's Hospital. Male C57BL/6 mice were purchased from Vital River Laboratory Animal Technology (Beijing, China). All mice were housed in a room at 22°C, with 55% humidity and 12-h-cycle lighting. Five male *Macaca mulatta* (rhesus monkeys from the Institute of Laboratory Animal Sciences, Sichuan Academy of Medical Sciences), 3 to 4 years of age, were used in this study. All monkeys were housed in a room at 22°C, with 12-h-cycle lighting and food provided three times daily.

Viral Vectors

scAAV2-EGFP (1×10^{12} vgs/mL) or scAAV2-C3 (5×10^{11} vgs/mL) (Figure 1A) was prepared by the Beijing FivePlus Molecular Medicine Institute (Beijing, China). scAAV2 vector expressed C3 or EGFP driven by a chicken beta-actin promoter combined with the CMV enhancer (CA). Briefly, the C3 gene (657 bp) or EGFP gene (720 bp) with restriction sites and pscAAV2-CA plasmid from Five-Plus molecular medicine institute (FMMI) were digested with KpnI/BglII (New England Biolabs, Ipswich, MA, USA) and linked to each other. Then the ligation products were transformed into *Escherichia coli* JM109 (Takara Bio, Dalian, China) for further replication and obtained the pscAAV2-CA-C3 or pscAAV2-CA-EGFP plasmid, which contained the AAV2 inverted terminal repeat (ITR) needed for the AAV package. scAAV2-CA-C3 or scAAV2-CA-EGFP vectors were prepared by triple transfection of HEK293T cells followed by purification using the method of chloroform treatment-polyethylene glycol (PEG)/NaCl precipitation-chloroform extraction as described previously.[60] A 0.22-μm polyvinylidene fluoride (PVDF) membrane filter (Merck Millipore, Billerica, MA, USA) provided sterilization. The viral titer was determined by qPCR method with the CA promoter as a target.

Cell Culture and Treatments

Primary HTM cells (ScienCell, Carlsbad, CA, USA) were cultured in TM Cell Medium (TMCM; ScienCell) at 37°C in an atmosphere of 5% CO_2, as previously described.[10,11,61] Cells of passages 3 to 4 were used in the experiments. For western blot experiments, HTM cells (1×10^6 cells per 25-cm^2 culture flask) were transduced with scAAV2-C3 (MOIs = 1.5×10^4 and 7.5×10^3) or scAAV2-EGFP (MOI = 1.5×10^4). For actin labeling, HTM cells were cultured to 100% confluence (4×10^5 cells per well in a 24-well plate) on coverslips, and then the cells were transduced with scAAV2-C3 or scAAV2-EGFP (MOI = 1.25×10^4). Images of morphology and EGFP expression were taken using an Olympus (Tokyo, Japan) CKX53 inverted fluorescence microscope.

Western Blot Analysis

Western blot assays were performed as described previously, with modification.[62] Membranes were immunoblotted with antibodies against RhoA (#2117, rabbit monoclonal antibody, 1:1,000; Cell Signaling Technology, Danvers, MA, USA) and GAPDH (AF5718, goat polyclonal antibody, 1 μg/mL; R&D Systems, Minneapolis, MN, USA).

Actin Labeling of HTM Cells and Tissues

Actin analyses of HTM cells, flat-mounted mouse corneas, and monkey eye sections (monkey 285) were performed with rhodamine-phalloidin (Cytoskeleton, Denver, CO, USA) staining.[11] Subsequently, the labeled tissues or HTM cells were imaged with a Leica TCS SP5 confocal laser scanning microscope (Wetzlar, Hesse, Germany).

Viral Delivery to the Anterior Segment

Each mouse was anesthetized with 4% chloral hydrate (0.1 mL/10 g body weight; Sigma-Aldrich, St. Louis, MO, USA) given intraperitoneally. scAAV2 suspension (0.5–1 μL) was delivered to the anterior chamber using a Hamilton glass syringe with a 33G needle (Hamilton, Reno, NV, USA) as previously described.[63]

Intracameral injection into monkey eyes was performed as previously described.[11] The viral vector suspension (30–60 μL) was delivered to the anterior chamber using a Hamilton glass syringe (100-μL volume) with a 30G needle (Hamilton).

IOP Measurement

IOP readings of the conscious mice were measured using the TonoLab rebound tonometer (Icare Finland, Espoo, Finland). The mice were gently restrained by hand and trained to acclimate to the measurement procedure until stable readings were consistently achieved.

Measurements were taken at the same time of the day between 2 and 4 p.m. on day 0 (before injection) and day 7.

IOP readings of each monkey were measured as described previously.[11] Measurements were taken at the same time of the day between 2 and 4 p.m. on day 0 (before injection), day 3, and day 7 during the first week, once weekly from day 7 to day 147, fortnightly from day 147 to day 175, and then every 6 weeks for the rest of the experiment period. Three readings were obtained per eye for each time point, and the mean IOP value was calculated and recorded in millimeters of mercury (mmHg).

Clinical Examinations of the Eye

General status of the monkey eyes was casually captured using a smartphone camera. The anterior segments of animals were regularly examined with a slit lamp biomicroscope (S350, Shanghai MediWorks Precision Instruments, Hangzhou, China) and recorded with an attached camera (EOS 600D, Canon, Tokyo, Japan). The corneal clarity and anterior chamber cells and flare were evaluated post-injection.

The examination of monkey eyes using ultrasound biomicroscope (MD-300L, UBM, Tianjin Maida Medical Technology, Tianjin, China) was conducted as previously described.[11] Five images were captured for each monkey, and the CCT, a marker of corneal hydration and metabolism, was quantified using Adobe Photoshop CS5 (San Jose, CA, USA).

In Vivo GFP Expression

The fluorescent image system of a Micron IV Retinal Imaging Microscope (Phoenix Research Labs, Pleasanton, CA, USA) was used to evaluate EGFP expression in mouse and monkey eyes as previously described.[10,11]

Eye Enucleation and Processing

Mice were sacrificed by cervical dislocation at 21 days post-injection. Monkey 285 was anesthetized and euthanized with sodium pentobarbital (120 mg/kg) administrated by intraperitoneal injection at 77 days. The eyes were immediately enucleated for pathological analysis.

In monkey 285, small (1-mm^3) pieces of peripheral cornea for TEM were isolated, fixed in 2.5% neutral phosphate-buffered glutaraldehyde, and post-fixed with 1% osmium tetroxide in 0.1 M phosphate buffer (pH 7.4). The tissue pieces were dehydrated in a graded ethanol series and embedded in epoxy resin. Ultrathin sections were cut and stained with uranyl acetate and lead citrate. Two sections of each eye were examined.

Mouse eyes and other monkey eye tissues were fixed in a formaldehyde, acetic acid, and saline (FAS) fixative (Wuhan Servicebio, Wuhan, China), infiltrated with paraffin, cut in 4-μm sections, and stained with H&E. Part of the sections in monkey eye were stored at −80°C for later actin labeling.

In direct fluorescence and actin labeling of cornea flat mounts, mouse eyes were fixed in 4% paraformaldehyde for 2 h and rinsed in PBS. The sclera was dissected with a circumferential incision parallel to the limbus, followed by removal of the lens and iris. Four radial cuts were made from the center of the cornea to allow flattening of the tissue.

H&E staining sections and flat-mount corneas (direct fluorescence) were photographed with an Olympus CKX53 inverted fluorescence microscope and then analyzed by an experienced ophthalmic pathologist.

Statistics

SPSS 18 software (IBM, Chicago, IL, USA) was used for statistical analysis. Comparisons between two groups were analyzed using the two-tailed paired Student's t test. Comparisons of multiple groups were performed using one-way analysis of variance (ANOVA). Regression models were fitted to assess the relationship between the IOP ratio and the grade of corneal edema or CCT. Selection of the most appropriate model required a significant ($p < 0.05$) coefficient for each polynomial term coupled with the greatest possible r^2 (coefficient of determination). A p value of <0.05 is statistically significant. Data are presented as mean ± SEM.

AUTHOR CONTRIBUTIONS

J.T. designed and performed most of the experiments, analyzed the data, and wrote the manuscript. X.W. designed and conducted the experiments. S.C., F.H., D.Z., D.L., L.Z. and N.F. helped to perform the experiments. X.Z. analyzed the data and reviewed the manuscript. X.L. coordinated the study, conceived and designed the experimental plan, analyzed the data, and finalized the manuscript.

CONFLICTS OF INTEREST

The authors declare no competing interests.

ACKNOWLEDGMENTS

We thank the Institute of Laboratory Animal Sciences (Chengdu, Sichuan, China) for providing laboratory spaces to perform the studies. This study was supported by grants from the National Natural Science Foundation of China (grant nos. 81770924 and 81900829), the Sanming Project of Medicine in Shenzhen (grant no. SZSM201512045), and the Science and Technology Innovation Committee of Shenzhen (grant no. GJHZ20170314102535241).

REFERENCES

1. Jonas, J.B., Aung, T., Bourne, R.R., Bron, A.M., Ritch, R., and Panda-Jonas, S. (2017). Glaucoma. Lancet *390*, 2183–2193.

2. Ayyala, R.S., Chaudhry, A.L., Okogbaa, C.B., and Zurakowski, D. (2011). Comparison of surgical outcomes between canaloplasty and trabeculectomy at 12 months' follow-up. Ophthalmology *118*, 2427–2433.

3. Inazaki, H., Kobayashi, S., Anzai, Y., Satoh, H., Sato, S., Inoue, M., Yamane, S., and Kadonosono, K. (2017). One-year efficacy of adjunctive use of Ripasudil, a rho-kinase inhibitor, in patients with glaucoma inadequately controlled with maximum medical therapy. Graefes Arch. Clin. Exp. Ophthalmol. *255*, 2009–2015.

4. Kaneko, Y., Ohta, M., Isobe, T., Nakamura, Y., and Mizuno, K. (2017). Additive intraocular pressure-lowering effects of ripasudil with glaucoma therapeutic agents in rabbits and monkeys. J. Ophthalmol. *2017*, 7079645.

5. Toris, C.B., McLaughlin, M.A., Dworak, D.P., Fan, S., Havens, S., Zhan, G.L., Horan, N., and Prasanna, G. (2016). Effects of Rho kinase inhibitors on intraocular pressure and aqueous humor dynamics in nonhuman primates and rabbits. J. Ocul. Pharmacol. Ther. *32*, 355–364.

6. Yu, M., Chen, X., Wang, N., Cai, S., Li, N., Qiu, J., Brandt, C.R., Kaufman, P.L., and Liu, X. (2008). H-1152 effects on intraocular pressure and trabecular meshwork morphology of rat eyes. J. Ocul. Pharmacol. Ther. *24*, 373–379.

7. Honjo, M., Tanihara, H., Inatani, M., Kido, N., Sawamura, T., Yue, B.Y., Narumiya, S., and Honda, Y. (2001). Effects of rho-associated protein kinase inhibitor Y-27632 on intraocular pressure and outflow facility. Invest. Ophthalmol. Vis. Sci. *42*, 137–144.

8. Aktories, K., Wilde, C., and Vogelsgesang, M. (2004). Rho-modifying C3-like ADP-ribosyltransferases. Rev. Physiol. Biochem. Pharmacol. *152*, 1–22.

9. Liu, X., Hu, Y., Filla, M.S., Gabelt, B.T., Peters, D.M., Brandt, C.R., and Kaufman, P.L. (2005). The effect of C3 transgene expression on actin and cellular adhesions in cultured human trabecular meshwork cells and on outflow facility in organ cultured monkey eyes. Mol. Vis. *11*, 1112–1121.

10. Tan, J., Fan, N., Wang, N., Feng, B., Yang, M., Liu, G., Wang, Y., Zhu, X., Kaufman, P.L., Pang, I.H., and Liu, X. (2018). Effects of lentivirus-mediated C3 expression on trabecular meshwork cells and intraocular pressure. Invest. Ophthalmol. Vis. Sci. *59*, 4937–4944.

11. Tan, J., Liu, G., Zhu, X., Wu, Z., Wang, N., Zhou, L., Zhang, X., Fan, N., and Liu, X. (2019). Lentiviral vector-mediated expression of exoenzyme C3 transferase lowers intraocular pressure in monkeys. Mol. Ther. *27*, 1327–1338.

12. Rohrbeck, A., von Elsner, L., Hagemann, S., and Just, I. (2014). Binding of *Clostridium botulinum* C3 exoenzyme to intact cells. Naunyn Schmiedebergs Arch. Pharmacol. *387*, 523–532.

13. Buie, L.K., Rasmussen, C.A., Porterfield, E.C., Ramgolam, V.S., Choi, V.W., Markovic-Plese, S., Samulski, R.J., Kaufman, P.L., and Borrás, T. (2010). Self-complementary AAV virus (scAAV) safe and long-term gene transfer in the trabecular meshwork of living rats and monkeys. Invest. Ophthalmol. Vis. Sci. *51*, 236–248.

14. Zurawski, C.A., McCarey, B.E., van Rij, G., and Fernandes, A. (1989). Corneal biometrics of the rhesus monkey (*Macaca mulatta*). J. Med. Primatol. *18*, 461–466.

15. Tamm, E.R. (2009). The trabecular meshwork outflow pathways: structural and functional aspects. Exp. Eye Res. *88*, 648–655.

16. Last, J.A., Pan, T., Ding, Y., Reilly, C.M., Keller, K., Acott, T.S., Fautsch, M.P., Murphy, C.J., and Russell, P. (2011). Elastic modulus determination of normal and glaucomatous human trabecular meshwork. Invest. Ophthalmol. Vis. Sci. *52*, 2147–2152.

17. Tektas, O.Y., and Lütjen-Drecoll, E. (2009). Structural changes of the trabecular meshwork in different kinds of glaucoma. Exp. Eye Res. *88*, 769–775.

18. Ye, Y., Yang, Y., Cai, X., Liu, L., Wu, K., and Yu, M. (2016). Down-regulation of 14-3-3 zeta inhibits TGF-β1-induced actomyosin contraction in human trabecular meshwork cells through RhoA signaling pathway. Invest. Ophthalmol. Vis. Sci. *57*, 719–730.

19. Pattabiraman, P.P., Rinkoski, T., Poeschla, E., Proia, A., Challa, P., and Rao, P.V. (2015). RhoA GTPase-induced ocular hypertension in a rodent model is associated with increased fibrogenic activity in the trabecular meshwork. Am. J. Pathol. *185*, 496–512.

20. Hill, L.J., Mead, B., Thomas, C.N., Foale, S., Feinstein, E., Berry, M., Blanch, R.J., Ahmed, Z., and Logan, A. (2018). TGF-β-induced IOP elevations are mediated by RhoA in the early but not the late fibrotic phase of open angle glaucoma. Mol. Vis. *24*, 712–726.

21. Vittitow, J.L., Garg, R., Rowlette, L.L., Epstein, D.L., O'Brien, E.T., and Borrás, T. (2002). Gene transfer of dominant-negative RhoA increases outflow facility in perfused human anterior segment cultures. Mol. Vis. *8*, 32–44.

22. Borrás, T., Buie, L.K., Spiga, M.G., and Carabana, J. (2015). Prevention of nocturnal elevation of intraocular pressure by gene transfer of dominant-negative RhoA in rats. JAMA Ophthalmol. *133*, 182–190.

23. Ho, T.T., Merajver, S.D., Lapière, C.M., Nusgens, B.V., and Deroanne, C.F. (2008). RhoA-GDP regulates RhoB protein stability. Potential involvement of RhoGDIalpha. J. Biol. Chem. *283*, 21588–21598.

24. Borrás, T., Gabelt, B.T., Klintworth, G.K., Peterson, J.C., and Kaufman, P.L. (2001). Non-invasive observation of repeated adenoviral GFP gene delivery to the anterior segment of the monkey eye in vivo. J. Gene Med. *3*, 437–449.

25. Barraza, R.A., Rasmussen, C.A., Loewen, N., Cameron, J.D., Gabelt, B.T., Teo, W.L., Kaufman, P.L., and Poeschla, E.M. (2009). Prolonged transgene expression with lentiviral vectors in the aqueous humor outflow pathway of nonhuman primates. Hum. Gene Ther. *20*, 191–200.

26. Lee, E.S., Rasmussen, C.A., Filla, M.S., Slauson, S.R., Kolb, A.W., Peters, D.M., Kaufman, P.L., Gabelt, B.T., and Brandt, C.R. (2014). Prospects for lentiviral vector mediated prostaglandin F synthase gene delivery in monkey eyes in vivo. Curr. Eye Res. *39*, 859–870.

27. Liu, X., Brandt, C.R., Gabelt, B.T., Bryar, P.J., Smith, M.E., and Kaufman, P.L. (1999). Herpes simplex virus mediated gene transfer to primate ocular tissues. Exp. Eye Res. *69*, 385–395.

28. Ethier, C.R., Wada, S., Chan, D., and Stamer, W.D. (2004). Experimental and numerical studies of adenovirus delivery to outflow tissues of perfused human anterior segments. Invest. Ophthalmol. Vis. Sci. *45*, 1863–1870.

29. Xiang, Y., Li, B., Wang, J.M., Li, G.G., Zhang, H., Manyande, A., and Tian, X.B. (2014). Gene transfer to human trabecular meshwork cells in vitro and ex vivo using HIV-based lentivirus. Int. J. Ophthalmol. *7*, 924–929.

30. Loewen, N., Fautsch, M.P., Peretz, M., Bahler, C.K., Cameron, J.D., Johnson, D.H., and Poeschla, E.M. (2001). Genetic modification of human trabecular meshwork with lentiviral vectors. Hum. Gene Ther. *12*, 2109–2119.

31. Oh, D.J., Kang, M.H., Ooi, Y.H., Choi, K.R., Sage, E.H., and Rhee, D.J. (2013). Overexpression of SPARC in human trabecular meshwork increases intraocular pressure and alters extracellular matrix. Invest. Ophthalmol. Vis. Sci. *54*, 3309–3319.

32. Spiga, M.G., and Borrás, T. (2010). Development of a gene therapy virus with a glucocorticoid-inducible MMP1 for the treatment of steroid glaucoma. Invest. Ophthalmol. Vis. Sci. *51*, 3029–3041.

33. Borrás, T., Xue, W., Choi, V.W., Bartlett, J.S., Li, G., Samulski, R.J., and Chisolm, S.S. (2006). Mechanisms of AAV transduction in glaucoma-associated human trabecular meshwork cells. J. Gene Med. *8*, 589–602.

34. Bennett, J., Ashtari, M., Wellman, J., Marshall, K.A., Cyckowski, L.L., Chung, D.C., McCague, S., Pierce, E.A., Chen, Y., Bennicelli, J.L., et al. (2012). AAV2 gene therapy readministration in three adults with congenital blindness. Sci. Transl. Med. *4*, 120ra15.

35. Jacobson, S.G., Cideciyan, A.V., Ratnakaram, R., Heon, E., Schwartz, S.B., Roman, A.J., Peden, M.C., Aleman, T.S., Boye, S.L., Sumaroka, A., et al. (2012). Gene therapy for leber congenital amaurosis caused by RPE65 mutations: safety and efficacy in 15 children and adults followed up to 3 years. Arch. Ophthalmol. *130*, 9–24.

36. Bogner, B., Boye, S.L., Min, S.H., Peterson, J.J., Ruan, Q., Zhang, Z., Reitsamer, H.A., Hauswirth, W.W., and Boye, S.E. (2015). Capsid mutated adeno-associated virus delivered to the anterior chamber results in efficient transduction of trabecular meshwork in mouse and rat. PLoS ONE *10*, e0128759.

37. Lee, S.H., Sim, K.S., Kim, C.Y., and Park, T.K. (2019). Transduction pattern of AAVs in the trabecular meshwork and anterior-segment structures in a rat model of ocular hypertension. Mol. Ther. Methods Clin. Dev. *14*, 197–205.

38. Borrás, T., Buie, L.K., and Spiga, M.G. (2016). Inducible scAAV2.GRE.MMP1 lowers IOP long-term in a large animal model for steroid-induced glaucoma gene therapy. Gene Ther. *23*, 438–449.

39. Gruenert, A.K., Czugala, M., Mueller, C., Schmeer, M., Schleef, M., Kruse, F.E., and Fuchsluger, T.A. (2016). Self-complementary adeno-associated virus vectors improve transduction efficiency of corneal endothelial cells. PLoS ONE *11*, e0152589.

40. Wang, Y., Wang, Y., Yang, Q., Guo, L., Yin, Y., Fan, N., Zhou, X., Cai, S.P., Kaufman, P.L., and Liu, X. (2014). Neuroprotective effects of C3 exoenzyme in excitotoxic retinopathy. Exp. Eye Res. *125*, 128–134.

41. Lehmann, M., Fournier, A., Selles-Navarro, I., Dergham, P., Sebok, A., Leclerc, N., Tigyi, G., and McKerracher, L. (1999). Inactivation of Rho signaling pathway promotes CNS axon regeneration. J. Neurosci. *19*, 7537–7547.

42. Bertrand, J., Winton, M.J., Rodriguez-Hernandez, N., Campenot, R.B., and McKerracher, L. (2005). Application of Rho antagonist to neuronal cell bodies promotes neurite growth in compartmented cultures and regeneration of retinal ganglion cell axons in the optic nerve of adult rats. J. Neurosci. *25*, 1113–1121.

43. Winzeler, A.M., Mandemakers, W.J., Sun, M.Z., Stafford, M., Phillips, C.T., and Barres, B.A. (2011). The lipid sulfatide is a novel myelin-associated inhibitor of CNS axon outgrowth. J. Neurosci. *31*, 6481–6492.

44. Bertrand, J., Di Polo, A., and McKerracher, L. (2007). Enhanced survival and regeneration of axotomized retinal neurons by repeated delivery of cell-permeable C3-like Rho antagonists. Neurobiol. Dis. *25*, 65–72.

45. Monnier, P.P., Sierra, A., Schwab, J.M., Henke-Fahle, S., and Mueller, B.K. (2003). The Rho/ROCK pathway mediates neurite growth-inhibitory activity associated with the chondroitin sulfate proteoglycans of the CNS glial scar. Mol. Cell. Neurosci. *22*, 319–330.

46. Fehlings, M.G., Kim, K.D., Aarabi, B., Rizzo, M., Bond, L.M., McKerracher, L., Vaccaro, A.R., and Okonkwo, D.O. (2018). Rho inhibitor VX-210 in acute traumatic subaxial cervical spinal cord injury: design of the SPinal Cord Injury Rho INhibition InvestiGation (SPRING) Clinical Trial. J. Neurotrauma *35*, 1049–1056.

47. Wang, C., Song, S., Zhang, Y., Ge, Y., Fang, X., Huang, T., Du, J., and Gao, J. (2015). Inhibition of the Rho/Rho kinase pathway prevents lipopolysaccharide-induced hyperalgesia and the release of TNF-α and IL-1β in the mouse spinal cord. Sci. Rep. *5*, 14553.

48. Xiaolu, D., Jing, P., Fang, H., Lifen, Y., Liwen, W., Ciliu, Z., and Fei, Y. (2011). Role of p115RhoGEF in lipopolysaccharide-induced mouse brain microvascular endothelial barrier dysfunction. Brain Res. *1387*, 1–7.

49. Uchida, T., Honjo, M., Yamagishi, R., and Aihara, M. (2017). The anti-inflammatory effect of ripasudil (K-115), a Rho kinase (ROCK) inhibitor, on endotoxin-induced uveitis in rats. Invest. Ophthalmol. Vis. Sci. *58*, 5584–5593.

50. Martin, T., Möglich, A., Felix, I., Förtsch, C., Rittlinger, A., Palmer, A., Denk, S., Schneider, J., Notbohm, L., Vogel, M., et al. (2018). Rho-inhibiting C2IN-C3 fusion toxin inhibits chemotactic recruitment of human monocytes ex vivo and in mice in vivo. Arch. Toxicol. *92*, 323–336.

51. Xiong, W., Wu, D.M., Xue, Y., Wang, S.K., Chung, M.J., Ji, X., Rana, P., Zhao, S.R., Mai, S., and Cepko, C.L. (2019). AAV *cis*-regulatory sequences are correlated with ocular toxicity. Proc. Natl. Acad. Sci. USA *116*, 5785–5794.

52. Wang, W.H., Millar, J.C., Pang, I.H., Wax, M.B., and Clark, A.F. (2005). Noninvasive measurement of rodent intraocular pressure with a rebound tonometer. Invest. Ophthalmol. Vis. Sci. *46*, 4617–4621.

53. Martinez-de-la-Casa, J.M., Garcia-Feijoo, J., Vico, E., Fernandez-Vidal, A., Benitez del Castillo, J.M., Wasfi, M., and Garcia-Sanchez, J. (2006). Effect of corneal thickness on dynamic contour, rebound, and goldmann tonometry. Ophthalmology *113*, 2156–2162.

54. Dohadwala, A.A., Munger, R., and Damji, K.F. (1998). Positive correlation between Tono-Pen intraocular pressure and central corneal thickness. Ophthalmology *105*, 1849–1854.

55. von Spiessen, L., Karck, J., Rohn, K., and Meyer-Lindenberg, A. (2015). Clinical comparison of the TonoVet(®) rebound tonometer and the Tono-Pen Vet(®) applanation tonometer in dogs and cats with ocular disease: glaucoma or corneal pathology. Vet. Ophthalmol. *18*, 20–27.

56. Neuburger, M., Maier, P., Böhringer, D., Reinhard, T., and F Jordan, J. (2013). The impact of corneal edema on intraocular pressure measurements using Goldmann applanation tonometry, Tono-Pen XL, iCare, and ORA: an in vitro model. J. Glaucoma *22*, 584–590.

57. Lau, W., and Pye, D. (2011). Changes in corneal biomechanics and applanation tonometry with induced corneal swelling. Invest. Ophthalmol. Vis. Sci. *52*, 3207–3214.

58. Almasieh, M., and Levin, L.A. (2017). Neuroprotection in glaucoma: animal models and clinical trials. Annu. Rev. Vis. Sci. *3*, 91–120.

59. Lindén, C., Heijl, A., Jóhannesson, G., Aspberg, J., Andersson Geimer, S., and Bengtsson, B. (2018). Initial intraocular pressure reduction by mono- versus multitherapy in patients with open-angle glaucoma: results from the Glaucoma Intensive Treatment Study. Acta Ophthalmol. *96*, 567–572.

60. Li, M., Tang, Y., Wu, L., Mo, F., Wang, X., Li, H., Qi, R., Zhang, H., Srivastava, A., and Ling, C. (2017). The hepatocyte-specific HNF4α/miR-122 pathway contributes to iron overload-mediated hepatic inflammation. Blood *130*, 1041–1051.

61. Keller, K.E., Bhattacharya, S.K., Borrás, T., Brunner, T.M., Chansangpetch, S., Clark, A.F., Dismuke, W.M., Du, Y., Elliott, M.H., Ethier, C.R., et al. (2018). Consensus recommendations for trabecular meshwork cell isolation, characterization and culture. Exp. Eye Res. *171*, 164–173.

62. Kumkarnjana, S., Suttisri, R., Nimmannit, U., Sucontphunt, A., Khongkow, M., Koobkokkruad, T., and Vardhanabhuti, N. (2019). Flavonoids kaempferide and 4,2′-dihydroxy-4′,5′,6′-trimethoxychalcone inhibit mitotic clonal expansion and induce apoptosis during the early phase of adipogenesis in 3T3-L1 cells. J. Integr. Med. *17*, 288–295.

63. Li, G., Gonzalez, P., Camras, L.J., Navarro, I., Qiu, J., Challa, P., and Stamer, W.D. (2013). Optimizing gene transfer to conventional outflow cells in living mouse eyes. Exp. Eye Res. *109*, 8–16.